The effect of solid-phase composition on the drying behavior of Markermeer sediment

Barciela-Rial, Maria; van Paassen, Leon A.; Griffioen, Jasper; van Kessel, Thijs; Winterwerp, Johan C.

DOI
10.1002/vzj2.20028

Publication date
2020

Document Version
Final published version

Published in
Vadose Zone Journal

Received: 14 August 2019 | Accepted: 5 April 2020

DOI: 10.1002/vzj2.20028

Vadose Zone Journal

ORIGINAL RESEARCH ARTICLE

The effect of solid-phase composition on the drying behavior of Markermeer sediment

Maria Barciela-Rial[1,2] | **Leon A. van Paassen**[3] | **Jasper Griffioen**[4,5] | **Thijs van Kessel**[6] | **Johan C. Winterwerp**[1]

[1]Hydraulic Engineering, Faculty of Civil Engineering and Geosciences, Delft Univ. of Technology, Delft, the Netherlands

[2]Sustainable River Management Group, HAN Univ. of Applied Sciences, Arnhem, the Netherlands

[3]School for Sustainable Engineering and the Built Environment, Arizona State Univ., Tempe, AZ, USA

[4]Copernicus Institute of Sustainable Development, Faculty of Geosciences, Utrecht Univ., Utrecht, the Netherlands

[5]TNO Geological Survey of the Netherlands, PO Box 80015, TA, Utrecht, 3508, the Netherlands

[6]Deltares, PO Box 177, Delft, MH, 2600, the Netherlands

Correspondence
Maria Barciela-Rial, Hydraulic Engineering, Faculty of Civil Engineering and Geosciences, Delft Univ. of Technology, Delft, the Netherlands.
Email: m.barcielarial@tudelft.nl

Funding information
Nederlandse Organisatie voor Wetenschappelijk Onderzoek, Grant/Award Number: 850.13.031

Abstract

We studied the drying behavior of slurries of Markermeer sediments in the Netherlands having different solid compositions. Natural processes such as sand–mud segregation and oxidation of organic matter were mimicked to analyze the effect of changes in sediment composition. Evaporation experiments were performed with soft slurry samples using the Hyprop setup. Soil water retention curves (SWRCs) and hydraulic conductivity curves (HCCs) were determined as a function of the water ratio (WR, defined as volume of water/volume of solids). The sediment remained close to saturation until the end of the experiments. The Atterberg limits reduced significantly after sediment treatment involving drying at 50 °C, rewetting, and chemical oxidation. Furthermore, the oxidized sediment lost capacity to retain water. The SWRCs of sandy and oxidized clays were steeper, and fine-textured sediments showed large water ratios. At low matric suctions, the water retention capacity of the upper sediment samples containing more labile organic matter was larger than that of the sediment underneath. Clear correlations were found between van Genuchten parameters and the degree of degradation of the organic matter. The hydraulic conductivity of fine-textured samples with less labile organics was larger. The results give insight into the drying behavior of Markermeer sediment, currently used to build wetlands.

1 | INTRODUCTION

Sandy sediments are traditionally preferred for reclamation projects to minimize deformation after construction, as muddy sediments show significant settlement when consolidating and drying. However, sandy sediment is becoming more scarce (Vörösmarty et al., 2003). Therefore, fine sediments are increasingly being used for nature building

Abbreviations: FID, flame ionization detection; HCC, hydraulic conductivity curve; HI, hydrogen index; LL, liquid limit; NE, northeast; OI, oxygen index; OM, organic matter; SW, southwest; SWRC, soil water retention curve; TOC, total organic carbon; WR, water ratio; XRD, X-ray diffraction.

projects (Erwin, Miller, & Reese, 2007; Haliburton, 1978). The Marker Wadden is one of the first projects in the Netherlands to use fresh unconsolidated cohesive sediment for wetland construction.

The Marker Wadden is a Building with Nature (BwN; de Vriend, van Koningsveld, Aarninkhof, de Vries, & Baptist, 2015) project which aims to improve the ecosystem of Lake Markermeer in the Netherlands by creating a new wetland with slurries originating from lake bed sediments (Figure 1). These slurries are deposited in sand compartments.

The Markermeer is a lake with an average water depth of 3.6 m and a surface area of 680 km^2 (Rozari, 2009). The uppermost layer of the lake bed consists of a thin (~0.1 m) layer of soft silt (van Duin, 1992). Underneath the soft silt layer is a thick layer of Holocene deposits (clay, peat, or sand) (Rijkswaterstaat, 1995).

During dredging of the slurry and filling of the compartments, segregation and oxidation of the sediments may occur (Ganesalingam, Sivakugan, & Ameratunga, 2013; Van Olphen, 2016). After deposition, the sediment settles while losing water through self-weight consolidation. Once the fill material emerges above the water table, the slurry will dry because of evaporation and may ultimately desaturate. Furthermore, organic matter (OM) and inorganic minerals will oxidize when the sediment is exposed to air (Saaltink, Dekker, Griffioen, & Wassen, 2016). Due to the heterogeneous

Core Ideas

- The sample preparation for Hyprop device was adapted to study drying of slurries.
- The Hyprop device is an efficient way to study the drying of slurries.
- The stability of organic matter is a greater determining factor than the total amount.
- Clear correlation was found between degree of OM degradation and van Genuchten parameters.

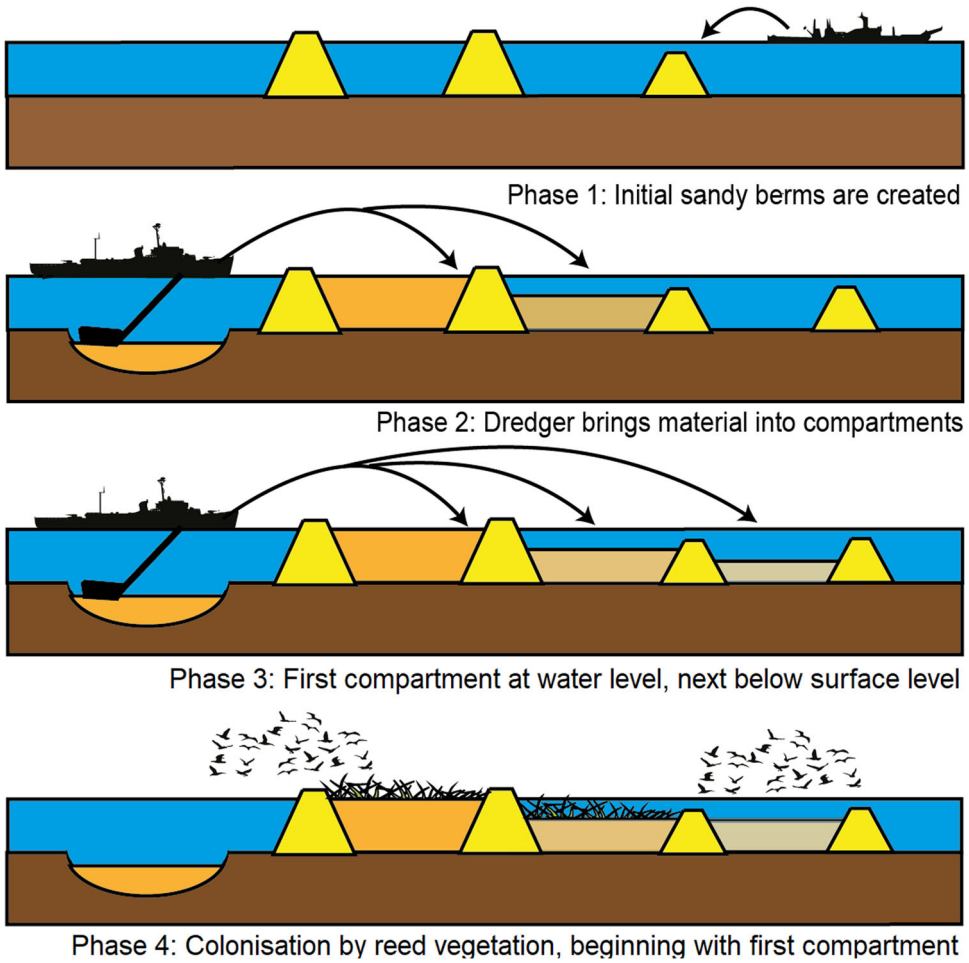

FIGURE 1 Method to build the artificial islands in the Marker Wadden wetland (adapted from Geretsen, 2014). Sand dams create compartments, of different heights, wherein the slurry is deposited. The new sediment, above and below water, will be used as habitat for flora and fauna

composition of the dredged Markermeer material and its spatial variability, the final properties of the sediment may be highly variable depending on initial composition, degree of oxidation, and environmental conditions.

The water balance of a drying soil is characterized by its soil water retention curve (SWRC) and the hydraulic conductivity curve (HCC). Various measurement techniques and empirically fitted models have been developed to determine the SWRC over the last decades (Fredlund, Rahardjo, & Fredlund, 2012; Lu & Likos, 2004). However, a measuring device that can determine the SWRC over the entire soil moisture range is not yet available (Schelle, Heise, Jänicke, & Durner, 2013). Therefore, it is common to construct composite curves using multiple techniques (ASTM, 2016). Once the water content–suction data are obtained experimentally, they may be analyzed with specific analytical functions such as those by Brooks and Corey (1964) and van Genuchten (1980).

In dewatering slurries, the majority of deformation takes place in the low ranges of suction. High-precision tensiometers may therefore be an appropriate tool for measuring pore water pressure. Using tensiometers, Wind (1968) developed an evaporation method, standardized by the ISO (2004b). Schindler and Müller (2006) modified and simplified this evaporation method by taking only measurements of mass and tension at two depths in a soil sample. Their method allows the simultaneous determination of the HCC. An increasingly popular and semiautomated version of this method is the Hyprop measurement system, commercialized by METER Group. This is the instrument used in the present paper because it replicates at small scale the drying conditions at the Marker Wadden while providing data to generate the SWRC and the HCC.

The SWRC and the HCC depend on the composition of the sediment. Notably, OM, particle size distribution, and soil texture strongly influence these curves. For instance, Rawls, Pachepsky, Ritchie, Sobecki, and Bloodworth (2003) found that the effect of OM on water retention differs between high and low organic C contents and depends on soil texture. Santagata, Bobet, Johnston, and Hwang (2008) related an increase of 8–10% in OM with a three- to fivefold increase in hydraulic conductivity of a normally consolidated soil. Tisdall and Oades (1982) and Chenu (1993) found that the water stability of soil microaggregates depends on characteristics of clay–OM interactions. However, most of the effort in linking OM to SWRC has focused on the amount of OM and not on the type or reactivity of OM.

In a similar line, other authors studied the effect of sand content on the behavior of clay–sand mixtures and the existence of a transitional fines content (TFC) threshold: at fine contents below the TFC, the behavior of the mixture changes from fine dominated to sand dominated (Simpson & Evans, 2016; Winterwerp & van Kesteren, 2004). Furthermore, some authors (Catana, Vanapalli, & Garga, 2006; Marinho, 2006) tried to find correlations between the rheological properties of the soils such as Atterberg limits and the SWRC. Although there is sufficient evidence for the impact of sand content and OM on hydrologic and rheological soil properties, the effect of the type of OM has not yet been studied. Further, the Hyprop approach has not been tested for clayey slurries.

The objective of this paper is to investigate the drying behavior of slurries with different solid composition with the Hyprop device. Using the Hyprop, SWRC and HCC were obtained from two tensiometer measurements and the continuous measurement of the weight of the sample. van Genuchten (1980) functions were fitted to the SWRC data. The sediment studied consisted of slurry samples from Lake Markermeer with varying sand and OM content. Furthermore, the effect of OM type and degree of maturity was also studied. To isolate the effect of different sediment fractions, several samples were manipulated prior to testing. For some samples, fines (<63 μm) were separated from coarse (>63 μm) grains. Other samples were dried, rewetted, and chemically oxidized. The goal of drying–rewetting and chemically oxidizing the samples was to accelerate aging of the sediments to compare this mimicked final behavior with the behavior of the original sediment of the bed. The study of hysteresis is beyond the scope of this study. The composition of the solid fraction of all samples was determined using various standard and nonstandard procedures prior to the Hyprop drying experiments.

2 | MATERIALS AND METHODS

2.1 | Sample collection and preparation

Sediment samples originated from Lake Markermeer, the Netherlands. Samples were taken from the uppermost soft silt layer and the underlying Holocene sediment. They were also collected from the bed of the lake with a Van Veen grab at two different locations: the southwest (SW) and the northeast (NE) sites, in the vicinity of the cities of Amsterdam and Lelystad, respectively (see Figure 2). The Holocene sediment from the SW site is referred to as clayey silt, and the one from the NE site is referred to as silty sand (see Table 1). The uppermost material at both sites was soft sandy silt. The sampled sediments were stored in dark conditions in a climate chamber at 4 °C.

The samples were tested whole and after sieving into fine (<63 μm) and coarse (>63 μm) fractions to determine the contribution of these size fractions to the soil properties of interest. Samples from both sites were pretreated, prior to the Hyprop test, to mimic the final natural remolded behavior of Markermeer sediment after drying–rewetting cycles and atmospheric oxidation of the OM. Since natural oxidation is slow, the oxidation process was accelerated in the

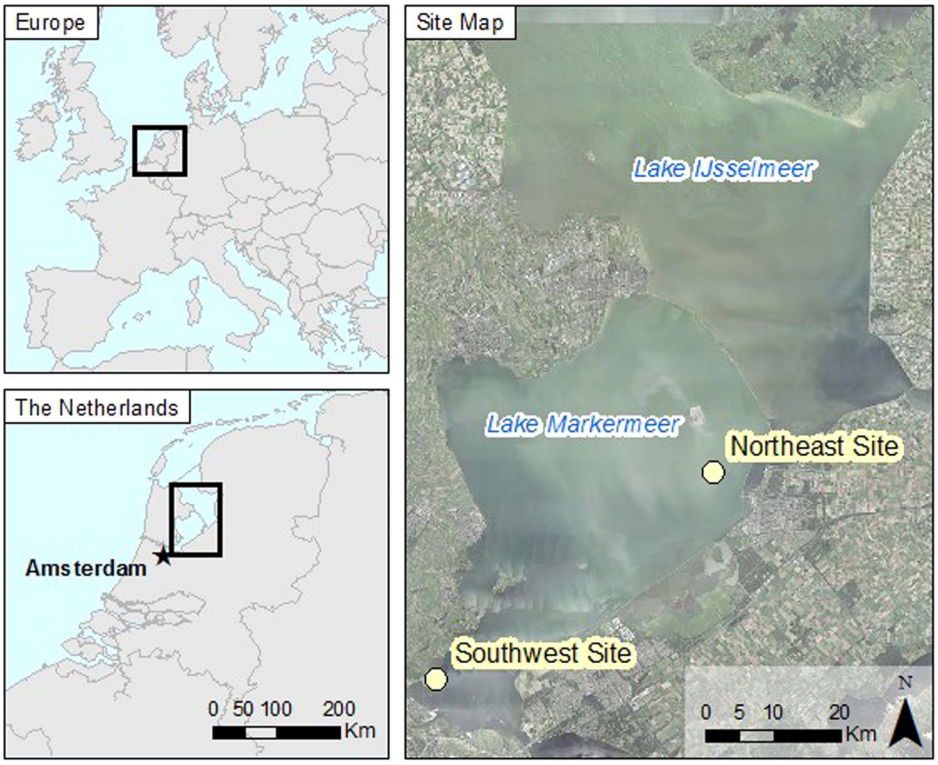

FIGURE 2 Location of the Markermeer (left) and study area with sampling sites (right). Source image: Publieke Dienstverlening Op de Kaart (PDOK) 2016

TABLE 1 Sample description: sampling sites, contents of different grain fractions, the cumulative 50% point of diameter (D50), total organic matter content (TOM), total organic C content (TOC), degradation oxygen/hydrogen index ratio (OI/HI), particle density (ρ_s), liquid limit (LL), plastic limit (PL), and plastic index (PI). Treated refers to chemically oxidized dried rewetted samples

Site	Depth	Type	ID	Sand	Silt	Clay	D50	TOM	TOC	OI/HI	ρ_s	LL	PL	PI
	m			——% mass——			μm	——%——			kg m^{-3}	——%——		
Southwest	0.1–0.5	Bulk clayey silt	SW1B	8	63	29	10	8.6	3.3	1.3	2,530	104	46	58
		Fines fraction	SW1F	0	69	31	8	8.7	3.1	1.4	2,570	129	59	70
		Bulk treated	SW1T	8†	63†	29†	10†	6.7	2.0	1.8	2,620	60	31	29
	0.0–0.1	Bulk soft sandy silt	SW2B	28	54	18	32	6.4	3.0	1.2	2,560	103	46	57
Northeast	0.0–0.1	Bulk soft sandy silt	NE1B	42	49	9	69	3.4	1.2	1.4	2,590	72	40	32
		Fines fraction	NE1F	0	86	14	26	4.8	2.0	1.0	2,540	83	49	34
		Bulk treated	NE1T	42†	49†	9†	69†	2.1	0.5	1.9	2,700	33	23	10
	0.1–0.5	Bulk silty sand	NE2B	69	21	10	87	2.1	0.7	1.6	2,640	41	25	16
		Sand fraction	NE2S	100	0	0	108	0.3	0.1	5.5	2,710	–	–	–

†Indicates assumed value, not measured for the sample

laboratory. Samples were chemically oxidized with 6% H_2O_2 solution, following an adapted procedure from the British Standards (1990b). The procedure included two drying–rewetting cycles. First, the samples were dried for ~1 wk in an oven at a constant temperature of 50 °C, until there was no more mass loss in a scale with accuracy 0.01 g. Then, subsamples of 100 g were rewetted by adding demineralized water and oxidized according to British Standards (1990b). When the oxidation process was complete, the oxidant (6% H_2O_2) was removed by centrifugation, also according to the standard. Afterwards, the material was dried again at 50 °C and finally rewetted with filtered Markermeer water. The filter had a size of 8–10 μm to remove plankton and other organics and floating woody debris. The pH was measured before and after oxidation by immersing a pH electrode in the samples.

2.2 | Sample characterization

2.2.1 | Analytical methods

The basic characterization included particle size distribution, total OM content, total organic C (TOC) content, particle density, and Atterberg limits. A gas pycnometer (ISO, 2014a) was used to measure the particle density, and the Atterberg limits were determined according to ISO (2004a).

The particle size distribution was determined for all dispersed (i.e., after immersion in dispersant solution overnight) natural samples by hydrometer and dry sieving according to British Standards (1990a). The particle size distribution of the treated samples was assumed to be the same as that of the original sample.

Total OM was determined according to EN (2012), whereas the amount and type of TOC was determined with the Rock Eval device (Behar, Beaumont, & De B. Penteado, 2001). The Rock Eval is a two-step process, which involves pyrolysis in an inert atmosphere and subsequent combustion in an oxic atmosphere. With this test, the amount of pyrolizable C and residual C were determined. The TOC was obtained as the sum of pyrolizable and residual C.

The pyrolizable C corresponds to the labile OM and comprises three major fractions: S1, S2, and S3. The S1 and S2 fractions were measured by flame ionization detection (FID). The S1 fraction (mg hydrocarbons g^{-1} sample) is composed of small volatile molecules. The S2 fraction (mg hydrocarbons g^{-1}) comprises larger, thermally cracked molecules of hydrocarbons. From this fraction, the hydrogen index (HI), which represents the relative importance of H-rich aliphatic compounds, is calculated. The S3 fraction is measured in milligrams of CO_2 per gram of dry sediment and comprises oxygen-containing organic molecules. Therefore, this S3 fraction is used to calculate the oxygen index (OI). The HI decreases, and the OI increases as the OM undergoes greater degradation and oxidation (Carrie, Sanei, & Stern, 2012; Disnar, Guillet, Keravis, Di-Giovanni, & Sebag, 2003).

The mineralogy of the bulk and clay fractions of the bulk natural and treated samples was determined by X-ray diffraction (XRD; Moore & Reynolds, 1989). Knowing the mineral composition was necessary prior to the design of the chemical oxidation to prevent drawbacks of the treatment, such as big drops in pH (Mikutta, Kleber, Kaiser, & Jahn, 2005). The composition was also needed to check whether the mineralogy was the same in both sampling sites, and whether the treatment affected the mineral composition.

2.2.2 | Sediment characterization

Results of the basic sediment characterization are shown in Table 1. The Atterberg limits of Markermeer sediments showed a decrease with increasing sand fraction and an increase with increasing TOC. This increase in Atterberg limits is due to the higher contents of OM and clay minerals binding water. Consequently, the materials from the SW site show higher Atterberg limits (Table 1). The H_2O_2 treatment decreased the liquid limit (LL) from 104 to 60% for sediment SW1B and from 72 to 33% for sediment NE1B. The plastic limit went from 46 to 31% for SW1B and from 40 to 23% for NE1B. Consequently, the sediment was able to hold less water. Sediment SW1T has a plasticity index below 30% and is classified as a medium plastic clay, whereas NE1T is just slightly plastic with a plasticity index of 10%.

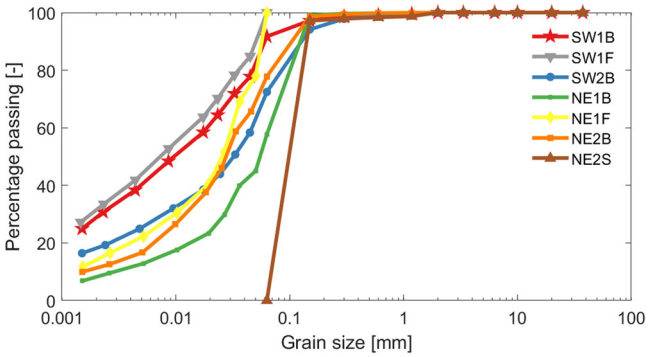

FIGURE 3 Particle size distribution of the various samples, determined by hydrometer and sieving. See Table 1 for definition of sample IDs

Figure 3 shows that the particle size distributions of the natural clay samples from the SW (samples SW1B and SW1F) and the NE (samples NE1B, NE1F and NE2B) differed, with the curves of the SW clay being less steep. Herein, the SW clay is less sandy than the NE clay. The upper part of the bed consisted of soft sandy silt and showed the presence of more shell fragments (carbonates) compared with deeper sediments. At the SW site, the upper soft sandy silt layer (SW2B) was coarser than the underlying clay layer, whereas the pattern for the NE is the opposite. The sand can be classified as fine for all samples (i.e., 0.063–0.15 mm according to ISO, 2016). The coarser particles all consisted of fragments of shells and large OM particles.

Figure 4 shows the Rock Eval results. The measured S1 curves for the soft silt from both sampling sites achieved larger maximum FID values than the underlying material. This implies that there are more volatile molecules present in the uppermost material (samples SW2B and NE1B) of the lake bed compared with the sediment underneath (samples SW1B and NE2B). Figure 4 also shows the subsequent S2 curve. Herein, the uppermost soft silt material of both sites (SW2B and SW1B) exhibited larger FID values at lower temperatures. Therefore, the S2 results also suggest that the OM in the top layer of the bed is more labile (i.e., reactive) at both sites. These differences in lability were also shown by

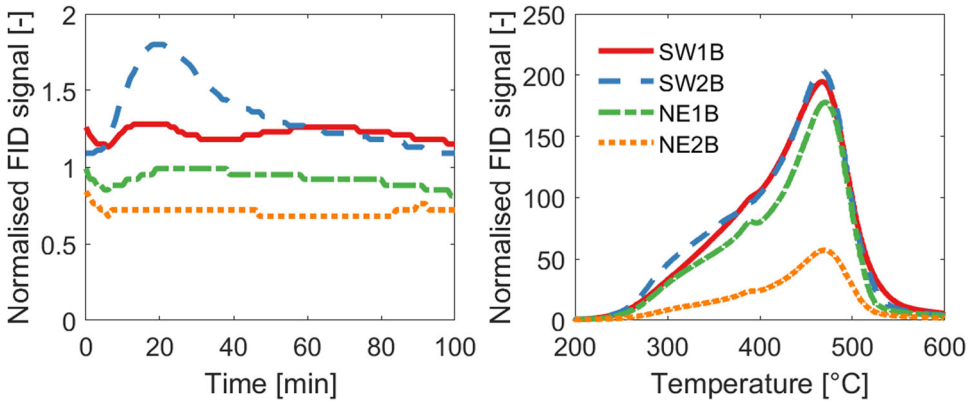

FIGURE 4 Rock Eval results for uppermost soft silt and deeper samples of both sites showing the S1 curve (volatile compounds, left) and the S2 curve (right). Vertical axis: flame ionization detection (FID signal). See Table 1 for definition of sample IDs

the OI/HI ratio (see Table 1). This ratio increased with the degree of degradation of the samples and thus exhibited the larger values for the treated samples. Despite the different lability, T_{max} (i.e., the temperature at which the peak in S2 curve occurred) was still the same for both materials. This indicates that their composition was still very similar.

The XRD analysis of the bulk mineralogical composition of the samples showed that all sediment types had a similar mineralogy, and that they mainly consisted of quartz (36.5–47.7%) and feldspar minerals (8.5–14.3%). The samples had considerable calcite contents (7–9%), which was the dominant carbonate. The calcite contents of Markermeer sediments were large enough to buffer pH (Hendriks, 2016). This was also shown by chemical oxidation of the samples, which lowered the pH of the sediment samples by only 0.4 units (from 7.9 to 7.5). From the oxides group, hematite was identified at relatively low contents (<1%). Pyrite was the dominant sulfide identified (which indicates in situ anoxic conditions), albeit at low contents (<1%).

Regarding the clay mineral fraction, the 2:1 phyllosilicates were the most abundant (13.0–35.6%). Herein, three types of 2:1 phyllosilicates were present: illite, smectite, and mixed illite–smectite layers. All samples had a similar clay fraction, including the treated samples. This shows that the applied treatment did not change the general sediment mineralogy.

2.3 | Evaporation experiments

2.3.1 | Methods

The Hyprop device (Figure 5) was used to determine the HCC and the SWRC properties of the slurries listed in Table 2. Slurries of the untreated samples were prepared at a water content lower than sampled in the field. The different samples were allowed to settle in storage containers to achieve the desired

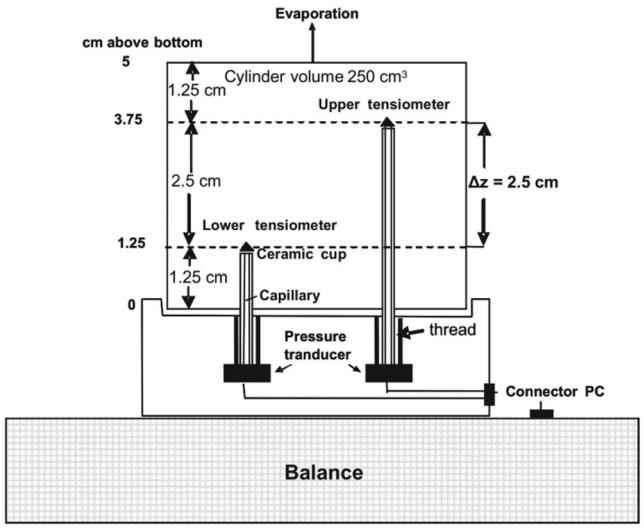

FIGURE 5 Schematic of the experimental Hyprop setup (after Schindler et al., 2010)

initial gravimetric water contents (w_0, M_w/M_s). The w_0 of all samples, listed in Table 2 was determine according to ISO (2014b) by oven drying. Table 2 also shows the initial bulk densities ($\rho_{b,0}$) and water ratios ($WR_0 = V_w/V_s$). To analyze the drying behavior at different initial water contents, replicates (I and II) were prepared at different w_0 for some samples. The treated samples were prepared at a water content of 1.5 times the LL. This water content was selected as being representative of the consistency at the end of self-weight consolidation for this sediment. After addition of water to attain the 1.5 LL water content, the samples were allowed to equilibrate for 48 h prior to testing. The 100% sand samples were prepared by first adding filtered Markermeer water to the container and then pouring in the sand. For each sediment sample, two evaporation experiments were performed (I and II), with the exception of the oxidized samples and the soft sandy

TABLE 2 Initial parameter values for the Hyprop evaporation experiments: initial water content (w_0), ratio w_0/liquid limie (LL), initial bulk density ($\rho_{b,0}$), and initial water ratio (WR_0), at the start of the experiment

	SW1B		SW1F		SW1T	SW2B		NE1B	NE1F		NE1T	NE2B		NE2S	
ID	Test I	Test II	Test I	Test II	–	Test I	Test II	–	Test I	Test II	–	Test I	Test II	Test I	Test II
w_0 (M_w/M_s)	1.4	2.1	5.1	2.6	0.9	1.8	1.9	0.9	3.8	2.0	0.5	0.7	0.7	0.3	0.3
w_0/LL, %	1.4	2.0	4.0	2.0	1.5	1.8	1.8	1.3	4.6	2.4	1.5	1.8	1.8	–	–
$\rho_{b,0}$, kg m^{-3}	1,318	1,226	1,106	1,170	1,492	1,271	1,260	1,294	1,150	1,222	1,683	1,537	1,527	1,977	1,949
WR_0 (V_w/V_s)	3.5	5.3	13.1	6.7	2.3	4.7	4.9	2.3	9.7	5.0	1.4	1.9	1.9	0.7	0.7

silt sample from the NE (NE1B), due to limited sediment availability.

The Hyprop device is based on the simplified evaporation method (Schindler & Müller, 2006). Hyprop consists is metallic cylindrical container with an inner diameter of 8 cm and a height of 5 cm enclosing a volume of 250 cm^3 of sediment sample. Balances with an accuracy of 0.01 g continuously monitored the mass loss of each sample during the evaporation experiments in a locked climate room at a constant temperature of 24 °C (±1 °C) and a relative humidity of 34% (±6%) while vibrations were prevented. The reproducibility of the results was tested by performing replicate experiments with identical samples at identical initial water contents. Two vertical ceramic tip tensiometers, with a diameter of 5 mm, were used to measure the suction pressures at 12.5 and 37.5 mm from the bottom of the sample. The tensiometers were previously filled with de-aired, demineralized water to improve accuracy, delay cavitation, and avoid retarded tensiometric measurements, as suggested by Durner and Or (2005).

For each sample, once the setup was installed (i.e., the ring and the tensiometers), the metallic container was filled gently with the slurry while avoiding air entrapment. A spoon was used to avoid trapping air in the sample when filling the Hyprop ring. The evaporation experiments were continued until both tensiometers cavitated, at which time the samples were removed from the container and dried in the oven at 105 °C to confirm the average water content. A computed tomography (CT) scan was performed to check that the sample filling method did yield homogenous samples.

2.3.2 | Suction measurements

Suction is defined as a positive pore water pressure, whereas hydrostatic pressures (i.e., the water pressure above atmospheric pressure) are negative. The measured pore water pressure is the result of multiple factors, such as the actual suction pressure, the hydrostatic pressure, the over–under pressure generated by sample preparation, potential self-weight consolidation, and an offset of the equipment (Tollenaar, 2017).

The tensiometer ceramic's air-entry value of 8,800 hPa was used as an additional measure of the slurry matric suction, following the extrapolation method of Schindler, Durner, von Unold, Müller, and Wieland (2010) and UMS (2015) to extend the measurement range. This additional value was used under the assumption that contact between the tensiometer and the soil is guaranteed until the air entry value is reached. Therefore, the 8,800-hPa point provides a measure of the water content corresponding to high suctions.

2.3.3 | Hydraulic conductivity curves

According to Schindler et al. (2010), the Hyprop setup can be used to determine the HCC. The unsaturated hydraulic conductivity, K, has traditionally been calculated according to Darcy–Buckingham's law, assuming quasi-steady-state (constant flux and hydraulic gradient) flow and a linearly decreasing water content across the sample height over the measuring interval (Equation 1; Schindler & Muller, 2006):

$$K(\overline{h}) = \frac{\Delta V}{2A\Delta t i_m} \tag{1}$$

where $\overline{h}$ is the mean hydraulic head, ΔV is the evaporated volume during the interval, A is the cross-sectional area, Δt is the time interval, and i_m is the hydraulic gradient. The hydraulic gradient is calculated according to

$$i_m = \frac{1}{2}\left(\frac{h_{t1,\text{upper}} - h_{t1,\text{lower}}}{\Delta z} + \frac{h_{t2,\text{upper}} - h_{t2,\text{lower}}}{\Delta z}\right) - 1 \tag{2}$$

where h refers to hydraulic head, $t1$ and $t2$ refer to two consecutive time steps, upper and lower refer to the upper and the lower tensiometer measurements, and Δz is the 2.5-cm vertical distance between the two tensiometers. Because some samples showed vertical shrinkage (for details, see Barciela-Rial, 2019), the above assumptions and equations were tested for the slurries studied. For this, the suction pressure difference between the upper and lower

tensiometer was determined. When the assumptions were valid, the two tensiometer measurements were used to calculate the hydraulic conductivity.

2.3.4 | Soil water retention curves

The SWRCs of the sediment are presented as a function of WR (V_w/V_s), as defined by Tollenaar, van Paassen, and Jommi (2018), instead of the traditional volumetric water content (V_w/V_t). Water ratio is preferred because of the large water content of the slurries studied.

Only the measured pressure of the lower tensiometer was used for the calculation of the SWRC, because the upper tensiometer emerged above the surface of the slurry in most tests, particularly for the clay samples because of their high initial water content. Further measurements with the upper tensiometer were then meaningless. The consistency between the two Hyprop tensiometers was investigated by Breitmeyer and Fissel (2017), who concluded that the Hyprop results obtained with either one (top or bottom) or two tensiometers were not statistically different. Therefore only the bottom tensiometer was used in this study.

3 | RESULTS AND DISCUSSION

3.1 | Suction measurements

The evaporation experiments with Hyprop provided tensiometer and mass loss data as output parameters. Figure 6 shows a typical example of the measured raw data. The suction pressure increased until cavitation started. The effect of self-weight consolidation on the measured suction pressure was very small (for details, see Barciela-Rial, 2019) and was neglected.

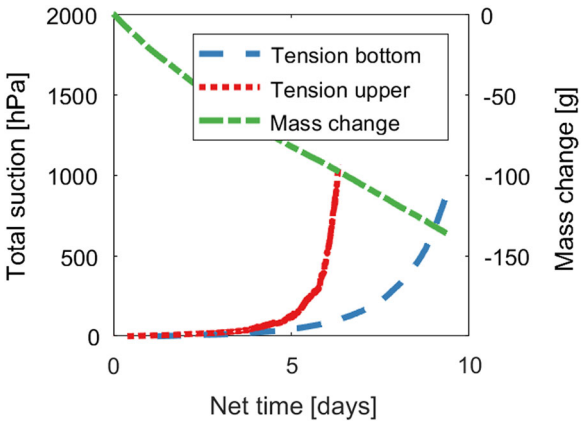

FIGURE 6 Raw upper and bottom tensiometer and weight change measurements for the bulk clayey silt SW1B-II sample

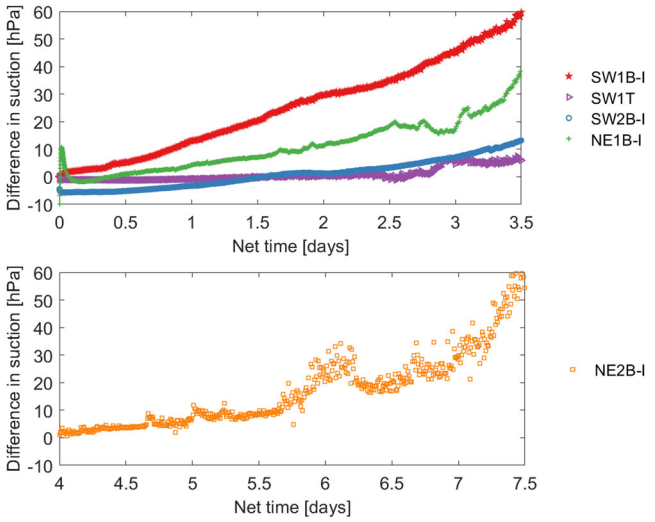

FIGURE 7 Suction pressure difference between the upper and lower tensiometer for the samples showing linear increase in the difference between suction at the upper and the lower tensiometer. Sample NE2B-I did not exhibit differences in suction during the first 4 d. See Table 1 for definition of sample IDs

3.2 | Hydraulic conductivity curves

For some samples with large initial water contents (samples SW1F and NE1F), the difference in suction between the upper and lower tensiometer remained constant during the first few days. The same was observed for the silty sand (NE2S) and for the treated sample with significant sand content (NE1T). After the few days, large suction gradients developed for all these samples (SW1F, NE1F, NE2S, and NE1T). Therefore, the assumptions of having linear gradients in the suction and water content were not met. These assumptions are necessary to calculate the hydraulic conductivity. This suggests that this method cannot be used to determine the hydraulic conductivity with the Hyprop for these samples. Furthermore, for samples SW1F and NE1F, the tensiometer protruded from the sample and could not be used.

Figure 7 shows the suction difference (an indication of the gradient) for the samples SW1B, SW1T, SW2B, NE1B, and NE2B for which the assumptions of quasi-steady-state and linear pressure gradient are considered valid. Figure 8 shows the results of the hydraulic conductivity (Equation 1) as a function WR for these samples. As expected, the hydraulic conductivity decreases with decreasing WR (increasing matric suction). The results suggest that samples with a larger OI/HI ratio (Table 1) have a larger hydraulic conductivity. This applies only to the samples whose behavior is not dominated by the sand fraction (Simpson & Evans, 2016): SW1B, SW2B, and SW1T. This highlights the importance of the type of OM determining the material properties for fine-textured sediment.

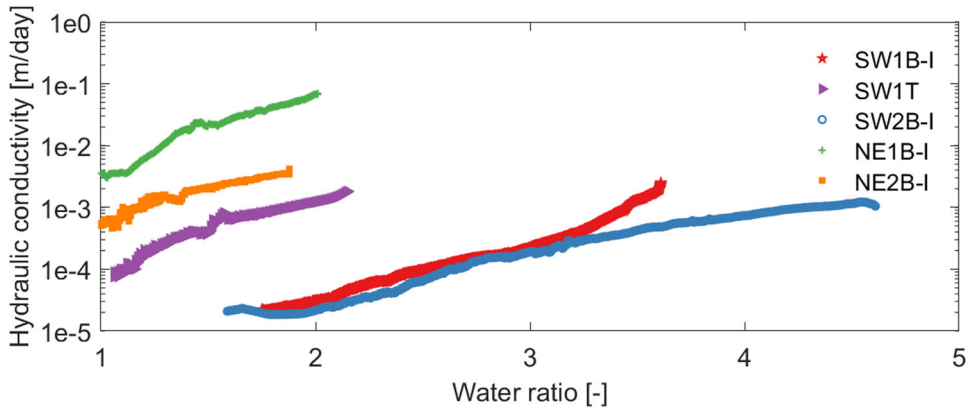

FIGURE 8 Hydraulic conductivity as a function of the water ratio of the samples meeting the requirements for the application of Darcy–Buckingham's law. See Table 1 for definition of sample IDs

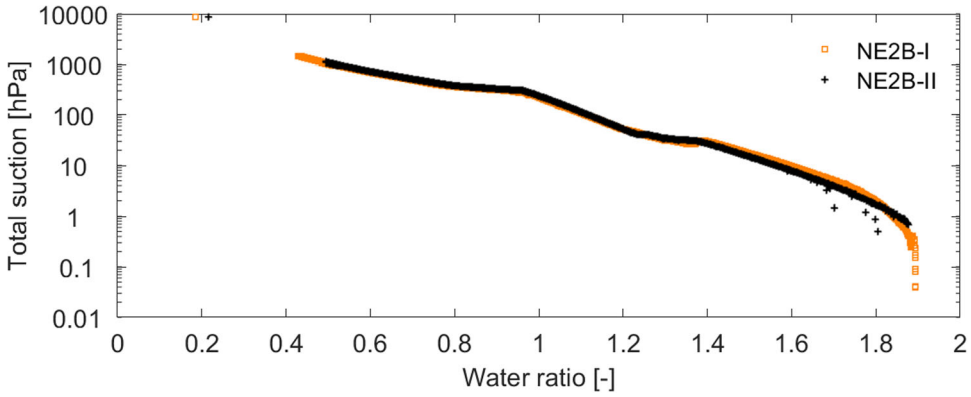

FIGURE 9 Water retention curves for replicates started at same initial water content for the NE2B sediment sample (i.e., silty sand with 69% sand). See Table 1 for definition of sample IDs

TABLE 3 Final gravimetric water contents (w_f) and water ratios (WR_f) at the end of the Hyprop tests

ID	SW1B		SW1F		SW1T	SW2B		NE1B	NE1F		NE1T	NE2B		NE2S	
	Test I	Test II	Test I	Test II	–	Test I	Test II	–	Test I	Test II	–	Test I	Test II	Test I	Test II
w_f (M_w/M_s)	0.36	0.43	4.47	0.40	0.23	0.30	0.73	0.13	0.27	0.47	0.07	0.07	0.08	0.01	0.01
WR_f (V_w/V_s)	0.91	1.08	1.21	1.02	0.60	0.78	1.86	0.77	0.69	1.20	0.18	0.19	0.22	0.02	0.02

3.3 | Soil water retention

Soil water retention curves were generated for all samples from the suction pressures and mass data. The SWRCs presented include an additional extrapolated point computed from the ceramic's air entry value. Figure 9 shows that the results presented in the current section are reproducible: two tests of identical samples show perfect overlap. Table 3 shows the gravimetric water content and WR at the end of the Hyprop experiments.

Although there was a difference in initial WR between (SW) replicate samples, the SWRCs converged at higher tension (Figure 10, left). Similar behavior is seen for the fines (Figure 10, right).

The samples exhibited different SWRCs, with the more coarse-textured samples (NE) showing lower initial WR and steeper SWRCs (Figure 11) in agreement with published data (Fredlund et al., 2012; Lu & Likos, 2004). For both sites, the upper samples (SW2B and NE1B) have higher WR than the lower samples (SW1B and NE2B). The different WR occurred only at the low suction range, as expected from the literature (Hillel, 2004), because of the different particle size distribution of the upper and lower samples. It is notable that the higher WR of the upper sediment is not just because it is coarser; in the NE site, the lower sample NE2B is coarser than the upper sample NE1B while having the same clay content. This suggests that the more labile OM present in the upper sandy silt layer (see Figure 4) has a larger influence on

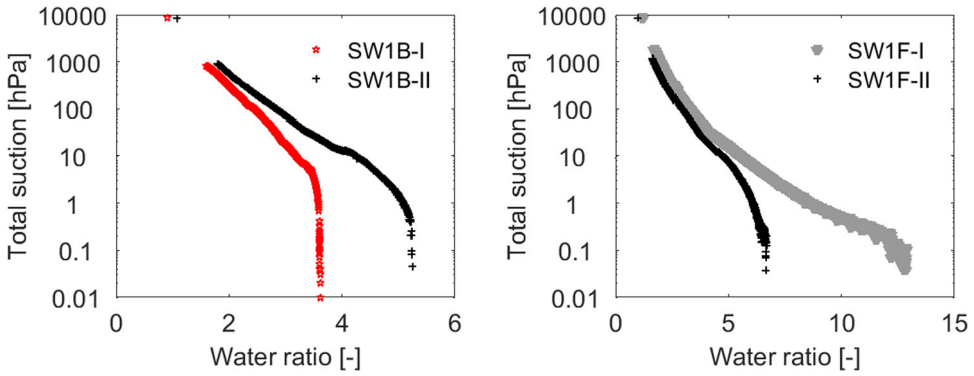

FIGURE 10 Water retention curves for replicates starting at different initial water content. Left panel, southwest (SW) bulk clayey silt. Right panel, SW fine fraction. Note the different horizontal scale. See Table 1 for definition of sample IDs

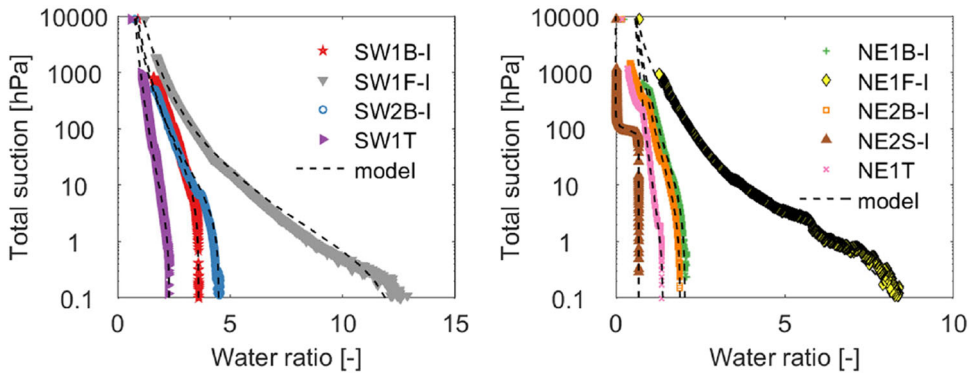

FIGURE 11 Comparison between experimental and model data for samples with a different sand content. Left panel, southwest (SW) samples. Right panel, northeast (NE) samples. Sand contents are 0% (SW1F-I and NE1F-I), 8% (SW1B-I), 28% (SW2B-I), 42% (NE1B-I), 69% (NE2B-I), and 100% (NE2S-I). See Table 1 for definition of sample IDs

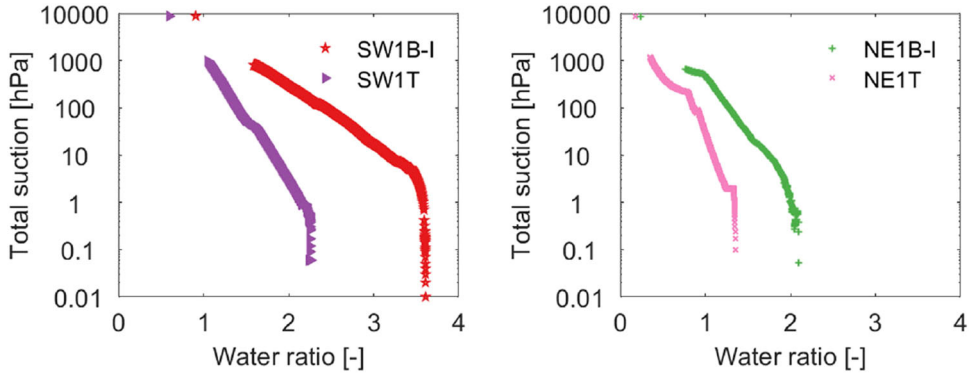

FIGURE 12 Water retention curves for natural and treated bulk clayey silt southwest (left) and sandy silt northeast (right) samples. See Table 1 for definition of sample IDs

increasing the WR than the coarser texture of the lower silty sand. Larger differences in WR between upper and lower samples are observed in the SW site because the upper sample SW2B does not only contain more labile OM but also has a coarser texture than the lower sediment.

The samples from both sites showed steeper SWRCs and lower initial WRs after treatment (Figure 12) because of the change in the aggregate structure and porosity caused by clay–OM bindings that disappear due to oxidation. Furthermore, the Atterberg limits showed a decrease in LL with decreasing OM, which shows an associated decrease in the ability to bind water (see also Zentar, Abriak, & Dubois, 2009). The results are in line with those of previous studies, such as Skempton (1969) and Burland (1990), who showed that the slope

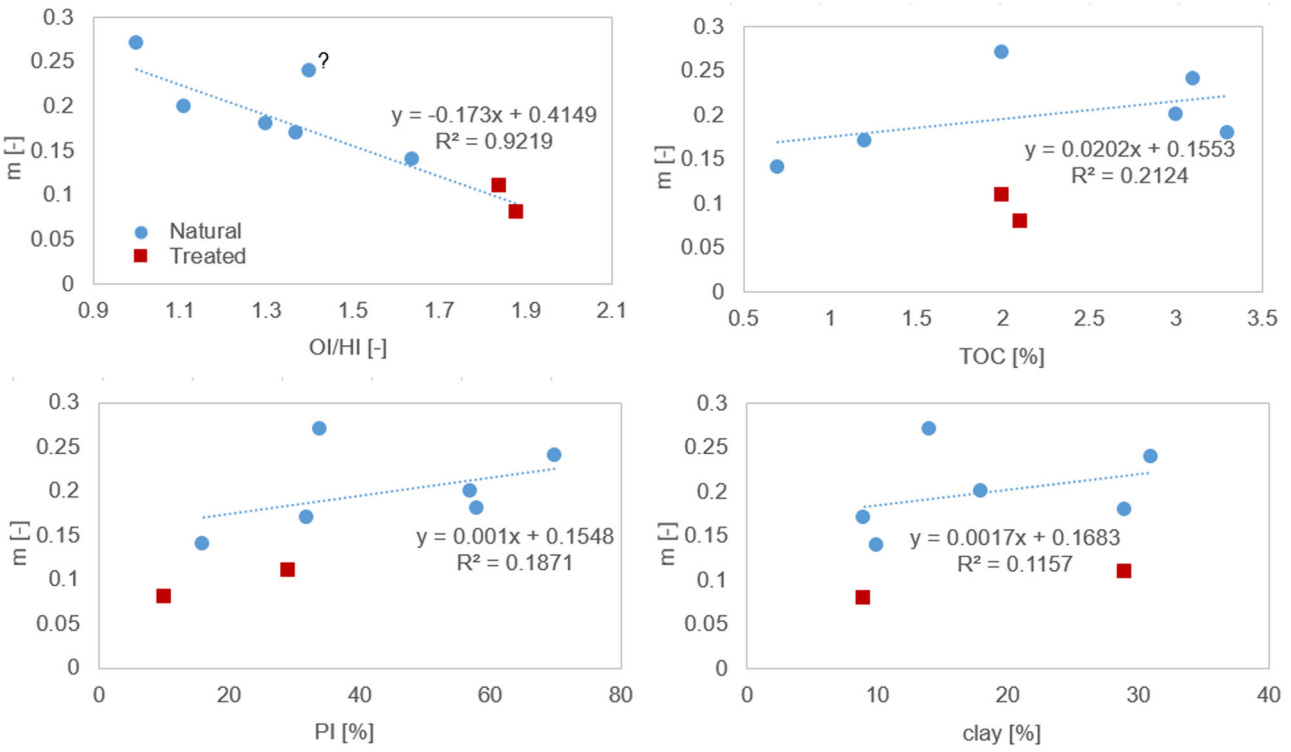

FIGURE 13 Correlation between the van Genuchten parameter *m* and different solid composition parameters (the oxygen/hydrogen index ratio [OI/HI], total organic C [TOC], plasticity index [PI], and clay percentage). The OI/HI value of sample SW1F was not accounted in the correlation shown (?). See Table 1 for definition of sample IDs

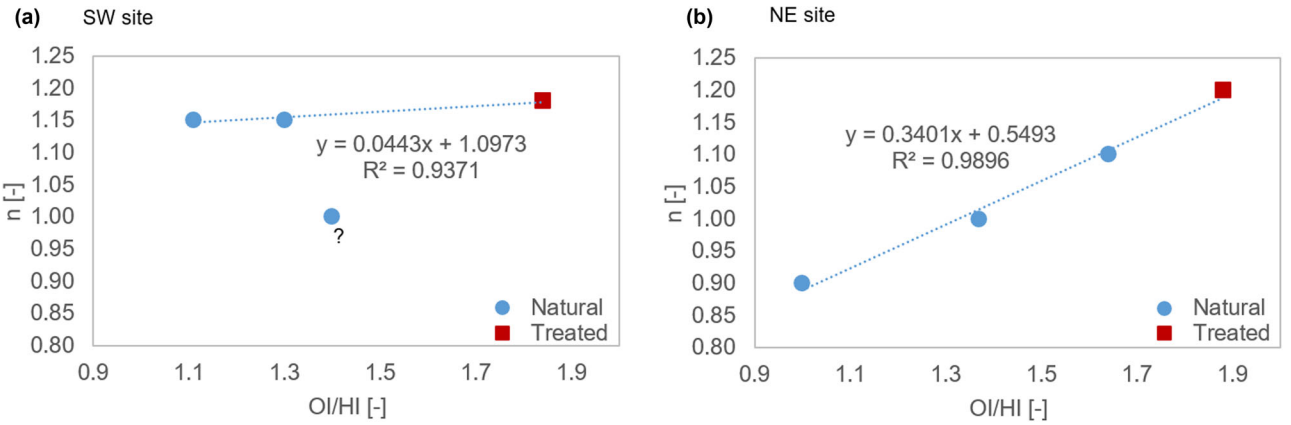

FIGURE 14 Correlation between the van Genuchten parameter *n* and the oxygen/hydrogen index ratio (OI/HI) for the southwest (SW, left) and northeast (NE, right) samples. The OI/HI value of sample SW1F was not accounted in the correlation shown (?). See Table 1 for definition of sample IDs

TABLE 4 Fitting parameters (α, *n*, and *m*), and correlation index (r^2) of the modeled soil water retention curve and standard deviation (σ) of the computed water ratio (WR) with respect to the experimental data

ID	SW1B Test I	SW1F Test I	SW1T –	SW2B Test I	NE1B –	NE1F Test I	NE1T –	NE2B Test I	NE2S Test I
α,hPa^{-1}	0.90	2.30	0.50	0.19	0.15	1.70	1.30	0.25	0.01
n	1.15	1.00	1.18	1.15	1.00	1.00	1.20	1.10	30.00
m	0.18	0.24	0.11	0.20	0.17	0.27	0.08	0.14	0.20
r^2	1.00	0.99	1.00	0.99	0.99	1.00	0.96	0.99	0.99
σ	0.14	0.44	0.04	0.14	0.05	0.18	0.15	0.14	0.04

of the compression curves, defining the compression index, experienced a similar dependency on sediment composition as observed in Figure 12. Santagata et al. (2008) also found a decrease in compressibility with a decrease in OM. The effect of OM on water retention properties has also been studied in other disciplines. Pons and Zonneveld (1965) described soils as a mixture of colloidal (fine OM and clay) and noncolloidal materials (silt, sand, and coarse OM). They interpreted ripening (as they defined the soil pedogenical processes) as a process involving a change in the microstructure of the clay minerals and the fine colloidal OM, together with a loss of water. In this sense, Figure 12 would give an indication of the differences in water retention behavior before and after ripening. Haynes (2005) pointed out that labile OM can be an indicator of soil quality that influences soil function. Consequently, for the case of the Marker Wadden wetland, the presence (and type) of OM also plays an ecological role on the development of the ecosystem at later stages.

3.4 | Modeling the soil water retention curve

The SWRCs were fitted with a van Genuchten model (van Genuchten, 1980) following Equation 3:

$$\mathrm{WR} = e_0\left[1 + (\alpha h)^n\right]^{-m} \tag{3}$$

where α (hPa^{-1}), n (–), and m (–) are fitting parameters, e_0 is the initial void ratio, h (hPa) is the suction head, and WR is the water ratio, which is equal to the void ratio at full saturation. Parameter α correlates to the inverse of the apparent air entry value of each curve, n correlates to the average slope of the water retention curve, and m correlates to the data for high suction. These free parameters were determined by best least squares fitting of Equation 3 to the complete range of experimental water content–suction data of each sample. Instead of linking the two parameters m and n to each other, following the original van Genuchten's proposal, they were kept independent (i.e., m is also a free parameter) to allow more flexibility in the calibration. This choice is justified by the assumption that parameter n is mainly dominated by capillarity and is therefore strongly dependent on soil structure (Hillel, 2004), whereas parameter m is dominated by the adsorption potential of the clay and the organic fractions (Lu & Khorshidi, 2015), reflecting a different retention mechanism.

The fitted parameters α, n, and m are shown in Table 4, and the comparison between the experimental data and the fitted curves is shown in Figure 11. Possible correlation between the parameter m and some index properties of the samples, namely the OI/HI, the TOC, the plasticity index, and the clay fraction (% clay), were evaluated after fitting the parameter onto the experimental data. The result is shown in Figure 13, which shows a very good correlation with the OI/HI ratio. The worse correlation being found with the total amount of organic content emphasizes the importance of the type of OM on the retention properties of the soil, in addition to the effect of the amount of OM and clay fraction.

Parameter n also showed a more clear correlation with the OI/HI ratio (Figure 14). Figure 14 shows this correlation for each sampling site. Analyzing each site separately was necessary because the parameter n describes the shape of the SWRC in the intermediate range of suctions, where capillarity dominates the response. Thus, the different particle size distributions found at the different sites (Figure 3) are expected to influence the results. Good correlation was found with the OI/HI ratio for each site independently, suggesting that the type of organic content also influences the fabric, and therefore the water retention dominated by capillarity.

4 | CONCLUSIONS

The effects of the type of OM and its oxidation, as well as sand content, on the hydrological properties of Markermeer sediment were evaluated. Samples were characterized, including determination of the OI/HI ratio with Rock Eval analysis to measure the lability of the OM. The soil water retention behavior was studied with an evaporation method using the Hyprop setup. This device proved to be a rapid and efficient method to evaluate the SWRC behavior of slurries. However, it showed limitations for obtaining the HCCs, especially for high initial WR. The results of samples meeting the requirements for HCC determination showed that fine-textured samples with a larger OI/HI ratio (i.e., lower lability) have a larger hydraulic conductivity.

The SWRC of sandy samples were steeper, and fine-textured sediments showed large WRs at all suctions. As expected, the differences in the water retention behavior were particularly large between the sample with 100% sand and those with 100% fines. In practice, this suggests that deformations or residual settlement may increase after deposition of the slurry layer if segregation occurs during the construction of the Marker Wadden. This may lead to large variability in the final sediment volumes. The WR capacity of the upper soft sandy silt layer was larger than that of the sediment layer underneath, particularly under conditions of low matric suction. This increase in WR is attributed to the difference in lability of the OM and is larger for the case of coarser textures. The effect of lability was also supported by the modeling of the SWRCs, where the van Genuchten parameters m and n were found to be more related to the type than the amount of OM.

The results show the importance of organic geochemical controls in the bulk physical properties of a clayey slurry. The present research showed the important physical implications of the lability of OM. Treating samples by

mimicking the exposure to oxidation and to drying and rewetting had a significant effect on water retention and a large reduction of the Atterberg limits. The water retention capacity and compressibility decreased, whereas the hydraulic conductivity increased after treatment. Therefore, the effect of oxidation and drying–rewetting should be considered when building new land with slurries, because the properties of the sediment may change significantly. However, future research on the effect of pretreatment may still be necessary, since the effects of drying and oxidation should be studied separately to gain further understanding.

ACKNOWLEDGMENTS

This study was supported with funding from the Netherlands Organization for Scientific Research (NWO, Project no. 850.13.031) and from Boskalis, Van Oord, Deltares, RoyalHaskoningDHV, and Natuurmonumenten. The authors would like to thank Cristina Jommi for her advice on the manuscript; Harry Veld, Roderick Tollenaar, and Arno Mulder for their support and advice during the performance of some of the experiments; and Nena Vandebroek for proofreading the manuscript.

CONFLICT OF INTEREST

The authors declare no conflict of interest.

REFERENCES

ASTM. (2016). *Standard test methods for determination of the soil water characteristic curve for desorption using a hanging column, pressure extractor, chilled mirror hygrometer, and/or centrifuge* (Method D6836-16). West Conshohocken, PA: ASTM International.

Barciela-Rial, M. (2019). *Consolidation and drying of slurries, a Building with Nature study for the Marker Wadden* (Doctoral dissertation). Delft, the Netherlands: Delft University of Technology.

Behar, F., Beaumont, V., & De B. Penteado, H. L. (2001). Rock-Eval 6 technology: Performances and developments. *Oil & Gas Science and Technology*, *56*, 111–134. https://doi.org/10.2516/ogst:2001013

Breitmeyer, R. J., & Fissel, L. (2017). Uncertainty of soil water characteristic curve measurements using an automated evaporation technique. *Vadose Zone Journal*, *16*(13). https://doi.org/10.2136/vzj2017.07.0136

British Standards Institution. (1990a). *Methods of test for soils for civil engineering purposes: Classification tests*. (Method BS 1377-2:1990). London: British Standards Institution.

British Standards Institution. (1990a). *Methods of test for soils for civil engineering purposes: General requirements and sample preparation* (Method BS 1377-1:1990). London: British Standards Institution.

Brooks, R. H., & Corey, A. T. (1964). *Hydraulic properties of porous media*. Fort Collins: Colorado State University.

Burland, J. B. (1990). On the compressibility and shear strength of natural clays. *Géotechnique*, *40*, 329–378. https://doi.org/10.1680/geot.1990.40.3.329

Carrie, J., Sanei, H., & Stern, G. (2012). Standardisation of Rock-Eval pyrolysis for the analysis of recent sediments and soils. *Organic Geochemistry*, *46*, 38–53. https://doi.org/10.1016/j.orggeochem.2012.01.011

Catana, M. C., Vanapalli, S. K., & Garga, V. K. (2006). The water retention characteristics of compacted clays. In G. A. Miller, C. E. Zapata, S. L. Houston, & D. G. Fredlund (Eds.), *Unsaturated soils* (pp. 1348–1359). Reston, VA: American Society of Civil Engineers. https://doi.org/10.1061/40802(189)111

Chenu, C. (1993). Clay- or sand-polysaccharide associations as models for the interface between micro-organisms and soil: Water related properties and microstructure. *Geoderma*, *56*, 143–156. https://doi.org/10.1016/0016-7061(93)90106-U

de Vriend, H. J., van Koningsveld, M., Aarninkhof, S. G. J., de Vries, M. B., & Baptist, M. J. (2015). Sustainable hydraulic engineering through building with nature. *Journal of Hydro-Environment Research*, *9*, 159–171. https://doi.org/10.1016/j.jher.2014.06.004

Disnar, J. R., Guillet, B., Keravis, D., Di-Giovanni, C., & Sebag, D. (2003). Soil organic matter (SOM) characterization by Rock-Eval pyrolysis: Scope and limitations. *Organic Geochemistry*, *34*, 327–343. https://doi.org/10.1016/S0146-6380(02)00239-5

Durner, W., & Or, D. (2005). *Soil water potential measurement*. In M. G. Anderson & J. J. McDonnell (Eds.), *Encyclopedia of hydrological science* (pp. 1089–1102). Hoboken, NJ: John Wiley & Sons.

Erwin, R. M., Miller, J., & Reese, J. G. (2007). Poplar Island Environmental restoration projects: Challenges in waterbird restoration on an island in Chesapeake Bay. *Ecological Restoration*, *25*(4). https://doi.org/10.3368/er.25.4.256

European Norm (EN) (2012). *Sludge, treated biowaste, soil and waste: Determination of loss on ignition (EN 15935)*. Brussels: European Committee for Standardization.

Fredlund, D. G., Rahardjo, H., & Fredlund, M. D. (2012). *Unsaturated soil mechanics in engineering practice*. Hoboken, NJ: John Wiley & Sons. https://doi.org/10.1002/9781118280492

Ganesalingam, D., Sivakugan, N., & Ameratunga, J. (2013). Influence of settling behavior of soil particles on the consolidation properties of dredged clay sediment. *Journal of Waterway, Port, Coastal, and Ocean Engineering*, *139*, 295–303. https://doi.org/10.1061/(ASCE)WW.1943-5460.0000183

Geretsen, P. (2014). *Design research Houtribdijk Marker Wadden*. Papendrecht, the Netherlands: Vista Svasek Hydraulics.

Haliburton, T. A. (1978). *Guidelines for dewatering/densifying confined dredged material*. Vicksburg, MS: U.S. Army Engineer, Waterways Experiment Station Environmental Laboratory.

Haynes, R. J. (2005). Labile organic matter fractions as central components of the quality of agricultural soils: An overview. *Advances in Agronomy*, *85*, 221–268. https://doi.org/10.1016/S0065-2113(04)85005-3

Hendriks, E. (2016). *The effect of pH and the solids composition on the settling and self-weight consolidation of mud* (Master's thesis). Delft, the Netherlands: Delft University of Technology.

Hillel, D. (2004). *Introduction to environmental soil physics*. Amsterdam: Elsevier Academic Press.

International Organisation for Standardisation (ISO). (2004a). Geotechnical investigation and testing—Laboratory testing of soil—Part 12: Determination of Atterberg limits (ISO/TS 17892-12:2004). Geneva: ISO.

International Organisation for Standardisation (ISO). (2004b). *Soil quality—Determination of unsaturated hydraulic conductivity and water-retention characteristic—Wind's evaporation method* (ISO 11275:2004). Geneva: ISO.

International Organisation for Standardisation (ISO). (2014a). *Determination of density by volumetric displacement: Skeleton density by gas pycnometry* (ISO 12154:2014). Geneva: ISO.

International Organisation for Standardisation (ISO). (2014b). *Geotechnical investigation and testing—Laboratory testing of soil- Part 1: Determination of water content* (ISO/TS 17892-1:2014). Geneva: ISO.

International Organisation for Standardisation (ISO). (2016). *Geotechnical investigation and testing—Laboratory testing of soil—Part 4: Determination of particle size distribution* (ISO 17892-4:2016.) Geneva: ISO.

Lu, N., & Khorshidi, M. (2015). Mechanisms for soil-water retention and hysteresis at high suction range. *Journal of Geotechnical and Geoenvironmental Engineering*, *141*(8). https://doi.org/10.1061/(ASCE)GT.1943-5606.0001325

Lu, N., & Likos, W. J. (2004). *Unsaturated soil mechanics*, Wiley, New York.

Marinho, F. A. M. (2006). A method of estimating the soil-water retention curve for plastic soils. In G. A. Miller, C. E. Zapata, S. L. Houston, & D. G. Fredlund (Eds.), *Unsaturated soils* (pp. 1473–1481). Reston, VA: American Society of Civil Engineers. https://doi.org/10.1061/40802(189)122

Mikutta, R., Kleber, M., Kaiser, K., & Jahn, R. (2005). Review: Organic matter removal from soils using hydrogen peroxide, sodium hypochlorite, and disodium peroxodisulfate. *Soil Science Society of America Journal*, *69*, 120–135. https://doi.org/10.2136/sssaj2005.0120

Moore, D. M., & Reynolds, J. R. C. (1989). *X-ray diffraction and the identification of clay minerals*. Oxford, UK: Oxford University Press.

Pons, L. J., & Zonneveld, I. S. (1965). *Soil ripening and soil classification: Initial soil formation in alluvial deposits and a classification of the resulting soils*. Wageningen, the Netherlands: International Institute for Land Reclamation and Improvement.

Rawls, W. J., Pachepsky, Y. A., Ritchie, J. C., Sobecki, T. M., & Bloodworth, H. (2003). Effect of soil organic carbon on soil water retention. *Geoderma*, *116*, 61–76. https://doi.org/10.1016/S0016-7061(03)00094-6

Rijkswaterstaat. (1995). *Geologische en bodemkundige atlas van het Markermeer*. Lelystad: the Netherlands: Rijkswaterstaat IJsselmeergebied.

Rozari, P. De (2009). Sediments and nutrient dynamics in the Lake Markermeer, the Netherlands. *Indonesian Journal of Chemistry*, *9*, 62–69. https://doi.org/10.22146/ijc.21563

Saaltink, R., Dekker, S. C., Griffioen, J., & Wassen, M. J. (2016). Wetland eco-engineering: Measuring and modeling feedbacks of oxidation processes between plants and clay-rich material. *Biogeosciences*, *13*, 4945–4957. https://doi.org/10.5194/bg-13-4945-2016

Santagata, M., Bobet, A., Johnston, C., & Hwang, J. (2008). One-dimensional compression behavior of a soil with high organic matter content. *Journal of Geotechnical and Geoenvironmental Engineering*, *134*, 1–13. https://doi.org/10.1061/(ASCE)1090-0241(2008)134:1(1)

Schelle, H., Heise, L., Jänicke, K., & Durner, W. (2013). Water retention characteristics of soils over the whole moisture range: A comparison of laboratory methods. *European Journal of Soil Science*, *64*, 814–821. https://doi.org/10.1111/ejss.12108

Schindler, U., Durner, W., von Unold, G., Müller, L., & Wieland, R. (2010). The evaporation method: Extending the measurement range of soil hydraulic properties using the air-entry pressure of the ceramic cup. *Journal of Plant Nutrition and Soil Science*, *173*, 563–572. https://doi.org/10.1002/jpln.200900201

Schindler, U., & Müller, L. (2006). Simplifying the evaporation method for quantifying soil hydraulic properties. *Journal of Plant Nutrition and Soil Science*, *169*, 623–629. https://doi.org/10.1002/jpln.200521895

Simpson, D. C., & Evans, T. M. (2016). Behavioral thresholds in mixtures of sand and kaolinite clay. *Journal of Geotechnical and Geoenvironmental Engineering*, *142*, 1–10. https://doi.org/10.1061/(ASCE)GT.1943-5606.0001391.

Skempton, A. W. (1969). The consolidation of clays by gravitational compaction. *Quarterly Journal of the Geological Society*, *125*, 373–411. https://doi.org/10.1144/gsjgs.125.1.0373

Tisdall, J. M., & Oades, J. M. (1982). Organic matter and water-stable aggregates in soils. *Journal of Soil Science*, *33*, 141–163. https://doi.org/10.1111/j.1365-2389.1982.tb01755.x

Tollenaar, R. N. (2017). *Experimental investigation on the desiccation and fracturing of clay* (Doctoral dissertation). Delft, the Netherlands: Delft University of Technology.

Tollenaar, R., van Paassen, L. A., & Jommi, C. (2018). Small scale evaporation tests on a clay: Influence of drying rate on a clayey soil layer. *Canadian Geotechnical Journal*, *55*, 437–445. https://doi.org/10.1139/cgj-2017-0061

UMS. (2015). *Manual HYPROP, version 2015-01*. Munich, Germany: UMS.

van Duin, E. H. S. (1992). *Sediment transport, light and algal growth in the Markermeer* (Doctoral dissertation). Wageningen, the Netherlands: Agricultural University.

van Genuchten, M. Th. (1980). A closed-form equation for predicting the hydraulic conductivity of unsaturated soils. *Soil Science Society of America Journal*, *44*, 892–898. https://doi.org/10.2136/sssaj1980.03615995004400050002x

van Olphen, E. J. C. (2016). *Consolidation behaviour of soft cohesive soils, the correlation between different scale model tests: Case study of the Marker Wadden* (Master's thesis). Delft, the Netherlands: Delft University of Technology.

Vörösmarty, C. J., Meybeck, M., Feteke, B., Sharma, K., Green, P., & Syvitski, P. M. (2003). Anthtorpogenic sediment retention; major global impact from registered river impoundments. *Global and Planetary Change*, *39*, 169–190. https://doi.org/10.1016/S0921-8181(03)00023-7

Wind, G. P. (1968). Capillary conductivity data estimated by a simple method. *Water in the Unsaturated Zone*, *1*, 181–191.

Winterwerp, J. C., & van Kesteren, W. G. M. (2004). *Introduction to the physics of cohesive sediment in the marine environment*. Amsterdam: Elsevier.

Zentar, R., Abriak, N. E., & Dubois, V. (2009). Fall cone test to characterize shear strength of organic sediments. *Journal of Geotechnical & Geoenvironmental Engineering*, *135*, 153–157. https://doi.org/10.1061/(ASCE)1090-0241(2009)135:1(153)

How to cite this article: Barciela-Rial M, van Paassen LA, Griffioen J, van Kessel T, Winterwerp JC. The effect of solid-phase composition on the drying behavior of Markermeer sediment. *Vadose Zone Journal*. 2020;19:e20028. https://doi.org/10.1002/vzj2.20028